

Article

Effects of Composition Variations on Mechanochemically Synthesized Lithium Metazirconate-Based Ceramics and Their Resistance to External Influences

Baurzhan K. Abyshev ^{1,2,*}, Sholpan G. Giniyatova ¹ and Artem L. Kozlovskiy ^{1,3} 

¹ Engineering Profile Laboratory, L.N. Gumilyov Eurasian National University, Satpayev St., Astana 010008, Kazakhstan; giniyatova_shg@enu.kz (S.G.G.)

² Nuclear Medicine Center, Medical Center Hospital of the President's Affairs Administration of the Republic of Kazakhstan, E495 Build No 2, Astana 010008, Kazakhstan

³ Laboratory of Solid State Physics, The Institute of Nuclear Physics, Almaty 050032, Kazakhstan

* Correspondence: baurzhan.abyshev@gmail.com; Tel./Fax: +77-024-4133-68

Abstract: The study examines the influence of variations in the compositions of components for the production of lithium-containing ceramics based on lithium metazirconate obtained by the method of mechanochemical grinding and subsequent thermal sintering. For component variation, two compositions were used, consisting of zirconium dioxide (ZrO_2) and two distinct types of lithium-containing materials: lithium perchlorate ($LiClO_4 \cdot 3H_2O$) and lithium carbonate (Li_2CO_3). Adjusting the concentration of these components allowed for the production of two-phase ceramics with varying levels of impurity phases. Using X-ray phase analysis methods, it was determined that the use of $LiClO_4 \cdot 3H_2O$ results in the formation of a monoclinic phase, Li_2ZrO_3 , with impurity inclusions in the orthorhombic phase, LiO_2 . On the other hand, when Li_2CO_3 is used, the resulting ceramics comprise a mixture of two phases, Li_2ZrO_3 and $Li_6Zr_2O_7$. During the studies, it was established that the formation of impurity inclusions in the composition of ceramics leads to an increase in the stability of strength properties with varying mechanical test conditions, as well as stabilization of thermophysical parameters and a decrease in thermal expansion during long-term high-temperature tests. It has been established that in the case of two-phase ceramics $Li_2ZrO_3/Li_6Zr_2O_7$ in which the dominance of the $Li_6Zr_2O_7$ phase is observed during high-temperature mechanical tests, a more pronounced decrease in resistance to cracking is observed, due to thermal expansion of the crystal lattice.

Keywords: lithium-containing ceramics; blankets; strength; thermal stability; phase transformations



Citation: Abyshev, B.K.; Giniyatova, S.G.; Kozlovskiy, A.L. Effects of Composition Variations on Mechanochemically Synthesized Lithium Metazirconate-Based Ceramics and Their Resistance to External Influences. *Ceramics* **2023**, *6*, 2394–2406. <https://doi.org/10.3390/ceramics6040147>

Academic Editor: Malika Saadaoui

Received: 14 October 2023

Revised: 2 December 2023

Accepted: 14 December 2023

Published: 15 December 2023



Copyright: © 2023 by the authors. Licensee MDPI, Basel, Switzerland. This article is an open access article distributed under the terms and conditions of the Creative Commons Attribution (CC BY) license (<https://creativecommons.org/licenses/by/4.0/>).

1. Introduction

The future progress of a country's energy sector will be closely tied to the adoption of alternative energy sources, with nuclear, hydrogen, and thermonuclear energy emerging as the most promising for substantial energy generation [1–3]. The expansion of their role in the energy sector is contingent not only on worldwide efforts to diminish reliance on fossil fuels and reduce harmful emissions but also on the imperative to bolster energy production capacity in response to growing energy demands from the populace [4,5]. One of the ways to solve the problems in the energy sector is to create new types of nuclear reactors, including high-temperature reactors, in which ceramic materials are to be used as core and nuclear fuel, as well as thermonuclear reactors based on technological solutions related to the production of energy from tritium. At the same time, to produce tritium, which, along with hydrogen, is one of the key types of nuclear fuel for thermonuclear installations, it is proposed to use lithium ceramics. Interest in lithium ceramics for the production of tritium is primarily due to the possibility of nuclear reactions involving the interaction of neutrons with lithium, which results in the formation of tritium, which can be used to support thermonuclear reactions and fuel production. At the same time, interest in the

development of ceramic materials containing lithium in this direction is primarily due to the possibility of creating sustainable materials for tritium multiplication (in order to maintain thermonuclear reactions), as well as those that are highly resistant to mechanical, thermal and radiation influences, which are integral factors accompanying the operation of ceramic materials.

A crucial aspect of ceramic production, or, in simpler terms, selecting a ceramic manufacturing method, involves examining the impact of manufacturing process variables and the specific procedures used in crafting ceramics [6–8]. The selection of these conditions plays a pivotal role in shaping the uniformity of the resultant ceramic compositions, along with a combination of physicochemical, structural, and thermophysical properties [9,10]. The methods currently available for obtaining lithium-containing ceramics can be categorized into several groups that share common technological processes. The most common method is the so-called melt method, combined with the sol-gel method, the use of which makes it possible to obtain spherical lithium-containing ceramics from compounds of lithium carbonate with zirconium, titanium or silicon oxides, depending on the type of ceramics that is planned to be obtained [11–15].

The aim of this work is to study the effect of component variations in the manufacture of lithium-containing ceramics based on lithium metazirconate on their phase composition, structural and strength characteristics, as well as stress resistance to temperature tests. The relevance of this work consists in the possibility of creating lithium-containing ceramics by mechanochemical synthesis with a controlled phase composition, which plays a very important role in determining the strength and thermophysical characteristics. Furthermore, the focus on ceramics based on lithium metazirconate primarily arises from its exceptional strength properties and its resistance to prolonged mechanical or radiation stress, along with its resistance to thermal expansion and degradation [16–20]. It is essential to emphasize that the objective of this study was not to produce single-phase ceramics but rather to precisely gauge the impact of impurity phases formed during mechanochemical mixing and subsequent thermal sintering on factors such as strength, thermophysical characteristics, thermal stability, and resistance to external influences [21–23]. This work is based on the hypothesis that the formation of impurity inclusions makes it possible to create additional barriers in ceramics for the propagation of microcracks under external influences, thereby increasing the strength of ceramics [24,25]. Moreover, since these inclusions also consist of the original components, this makes it possible to increase the concentration of lithium in the ceramic composition.

2. Materials and Research Methods

The synthesis of lithium-containing ceramics was carried out by using two types of compositions of the initial mixtures: (1) ZrO_2 and $LiClO_4 \cdot 3H_2O$ and (2) ZrO_2 and Li_2CO_3 with varying the molar ratio of the components from 0.25 to 0.75 M. In the future, these compositions will be designated as 1 and 2. The selection of these two compositions, featuring different components, stems from the potential to create lithium-containing ceramics with diverse phase compositions, strength, and thermophysical properties. Additionally, the choice of using $LiClO_4 \cdot 3H_2O$ and Li_2CO_3 as the lithium component was made to evaluate the feasibility of the mechanochemical synthesis method in producing stable ceramics with high lithium concentrations, which constitutes a crucial criterion when selecting ceramics for tritium production.

The primary approach employed to manufacture lithium-containing ceramics was the mechanochemical solid-phase synthesis method. This method entails mechanically blending the initial components within a PULVERISETTE 6 planetary mill (Fritsch, Berlin, Germany) for 5 h at a grinding speed of 300 rpm, with the aim of achieving a uniform particle size distribution. Subsequently, the resulting powders were compacted into 10 mm diameter and 1 mm thickness tablets, considering the requirements of the measuring instruments used to determine properties such as hardness, fracture resistance, and thermal conductivity. The tablets were pressed using a mold specially made for this purpose

under a pressure of 250 MPa. After pressing, the resulting tablets were subjected to thermal annealing at a temperature of 900 °C in a muffle furnace SNOL 39/1100 (AB UMEGA-GROUP, Ukmergė, Lithuania). Annealing was carried out for 8 h in an air atmosphere, followed by cooling for 24 h with the furnace. The selection of these annealing conditions, encompassing temperature, duration, and cooling process, was informed by prior experimental investigations [26,27], alongside a priori knowledge concerning phase and structural transformations in lithium-containing ceramics derived through mechanochemical or solid-phase synthesis.

The analysis of structural parameters and phase composition in the examined ceramics, contingent on the type of initial component composition and its variations, was conducted through an assessment of the X-ray diffraction patterns. These patterns were captured in the Bragg-Brentano configuration ($2\theta = 25\text{--}100^\circ$) with an increment of 0.03° . A Cu— α X-ray tube with a wavelength of 1.54 \AA was used as an X-ray source. The diffraction data was collected using a D8 Advance ECO X-ray diffractometer (Bruker, Berlin, Germany). The interpretation of the acquired diffraction patterns was facilitated by the Diffrac EVA v.4.2 software (Bruker, Berlin, Germany), enabling the determination of structural parameters such as crystal lattice dimensions, volume, and the structural order degree, along with the calculation of phase contributions within the samples. The weight contributions of each identified phase within the samples were ascertained by calculating the areas of all diffraction reflections characteristic of a given phase and then determining their ratio relative to other established phases. The degree of structural ordering (degree of crystallinity) was determined as the ratio of the contributions of the intensities of all diffraction reflections to the area of background radiation recorded during the angular dependence of the change in the intensity of X-ray diffraction patterns.

The mechanical properties, including alterations in hardness and resistance to cracking during a single compression, were evaluated for the investigated ceramics with regard to variations in their phase composition using established methods. Hardness assessments were conducted by applying a load of 100 N on a Vickers diamond pyramid indenter for 15 s, followed by the evaluation of the resultant indenter imprint on the sample. These experiments were carried out using a Duroline M1 microhardness tester (Metkon, Bursa, Turkey). The assessments of the hardening factors were based on the data concerning changes in hardness, attributable to adjustments in component ratios, as well as the introduction of impurity phases within the structure.

A single compression, based on the data of which the dynamics of changes in cracking with increasing pressure on the sample was established, was carried out using a mechanical testing machine LFM-L 10 kN (Walter + Bai AG, Leunigen, Switzerland). At the same time, to establish the effect of crack resistance when varying the compression rate, a series of experiments were carried out on samples in which the samples were subjected to compression at different compression rates. The influence of thermal expansion on crack resistance was determined by conducting experiments on single compression of samples heated in a chamber at a temperature of 500 °C.

Thermal conductivity coefficient measurements were conducted in the temperature range of 25 to 700 °C using the longitudinal heat flow method. The KIT-800 instrument from Teplofon, Moscow, Russia, was employed for these measurements.

The coefficient of thermal expansion for the ceramic samples, influenced by prolonged thermal exposure during 500 h of heating at 700 °C, was determined by assessing changes in the crystal lattice volume before and after thermal exposure. Using Formula (1), alterations in material properties due to high-temperature degradation were calculated based on the acquired data.

$$\beta_V(T) = \frac{1}{V_{\text{initial}}} \frac{\Delta V}{\Delta T}, \quad (1)$$

where ΔV is the change in the volume of the crystal lattice before and after high-temperature heating, ΔT is the difference in measurement temperatures, and V_{initial} is the volume of the crystal lattice of the initial sample. The crystal lattice volume was determined by

calculating the crystal lattice parameters for each test sample by analyzing the obtained X-ray diffraction patterns of the ceramic samples under study. Moreover, in the case of thermal tests, before they were carried out, the parameters and volume of the crystal lattice of each test sample were measured, after which, after thermal exposure, X-ray diffraction patterns were obtained, on the basis of which the parameters of the crystal lattice of the samples after thermal exposure were determined. Through comparative analysis, the values of changes in the volume of the crystal lattice were calculated, indicating changes in the properties of ceramics as a result of external influences.

3. Results and Discussion

In previous studies [28,29], it was demonstrated that modifications in the synthesis conditions, such as adjusting the proportions of the initial solution components, result in alterations in the ceramics' phase composition. This, in turn, directly influences the material's hardening effects and thermophysical properties. It is important to note that these studies explored the use of $\text{LiClO}_4 \cdot 3\text{H}_2\text{O}$ as a lithium-containing component. Changes in its concentration or variations in the thermal sintering conditions lead to the formation of impurity inclusions in the form of oxide phases. As indicated in [28], these inclusions enhance resistance to radiation-induced swelling during the accumulation of helium in the surface layer.

Figure 1 presents the X-ray diffraction results for the ceramic samples obtained from composition 1, with varying proportions of the components. These diffraction patterns reveal the impact of altering the initial component concentrations on the phase composition, specifically the changes in the relative amounts of the identified components within the samples. The X-ray diffraction data indicate that the primary phase in all three samples is the Li_2ZrO_3 (PDF-00-033-0843) monoclinic phase, and characteristic reflections of the LiO_2 (PDF-01-080-3472) orthorhombic phase are also detected. An analysis of the weight percentages of these phases, based on the determination of the weight ratio of the areas of diffraction reflections for each established phase, is detailed in Table 1. As per the provided data, an increase in the $\text{LiClO}_4 \cdot 3\text{H}_2\text{O}$ mixture composition results in a rise in the contribution of the LiO_2 impurity phase, increasing from 1.4 wt% to 5.7 and 7.3 wt%. Concurrently, the assessment of structural parameters, also depicted in Figure 2, signifies an improvement in the crystal lattice of the primary Li_2ZrO_3 phase, as evidenced by a reduction in the parameters and volume of the crystal lattice. Comparable alterations in structural parameters with variations in the component ratios are also observed for the LiO_2 impurity orthorhombic phase.

Analyzing the data obtained, we can conclude that when lithium perchlorate ($\text{LiClO}_4 \cdot 3\text{H}_2\text{O}$) is used as a lithium-containing component, the main phase in the ceramics is the monoclinic phase Li_2ZrO_3 . At the same time, at high concentrations of $\text{LiClO}_4 \cdot 3\text{H}_2\text{O}$ in the composition, the formation of the orthorhombic phase of LiO_2 in the form of inclusions is observed, the maximum content of which is no more than 7.3 wt%. Moreover, according to the data of works [28,29], the content of impurity inclusions, even in the case of varying thermal sintering conditions, does not exceed 10 wt%.

Therefore, upon examining the observed alterations in structural parameters, it can be deduced that as the concentration of $\text{LiClO}_4 \cdot 3\text{H}_2\text{O}$ increases, the ceramics become denser owing to the structural organization of the recognized phases. Furthermore, upon assessing the phase composition, an augmentation in the LiO_2 impurity phase within the ceramic composition was ascertained. This, in turn, can potentially impact modifications in the thermophysical and strength properties of the ceramics.

Figure 2 shows the data on changes in X-ray phase analysis of the studied ceramic samples obtained from composition 2 (in which Li_2CO_3 was used as a lithium-containing component). According to the assessment of structural parameters, as well as the shape and position of diffraction reflections, a change in the concentration of the Li_2CO_3 component (due to its increase in content) leads to more pronounced changes in the phase composition during mechanochemical stirring and subsequent thermal annealing. At a low

concentration of Li_2CO_3 in the ceramic composition, the presence of two monoclinic phases, Li_2ZrO_3 (PDF-00-033-0843) and $\text{Li}_6\text{Zr}_2\text{O}_7$ (PDF-01-081-2375), is observed. Simultaneously, the dominant phase, Li_2ZrO_3 , comprises over 90% of the composition. It is noteworthy that the close-to-symmetrical configuration of the diffraction reflections suggests a minimal presence of structural distortions within the structure. As the Li_2CO_3 concentration within the ceramic composition changes, there is a more than twofold surge in the $\text{Li}_6\text{Zr}_2\text{O}_7$ phase contribution in the composition when the component ratios in composition 2 are equal. It exhibits dominance, exceeding 80%, when the component ratio is 0.75 to 0.25. This shift in the phase composition signifies that the inclusion of Li_2CO_3 in the initial mixtures, followed by mechanochemical milling and subsequent thermal annealing, triggers phase transformation processes. These processes are linked to the transformation of the Li_2ZrO_3 phase into $\text{Li}_6\text{Zr}_2\text{O}_7$, all while preserving the structural motif and crystal lattice type. Simultaneously, an examination of the crystal lattice parameters and volume, as detailed in Table 2, highlights that the prevalence of $\text{Li}_6\text{Zr}_2\text{O}_7$ results in more pronounced structural ordering. The changes in lattice parameters and volume are more significant at concentrations of 0.75 to 0.25 than at other concentrations.

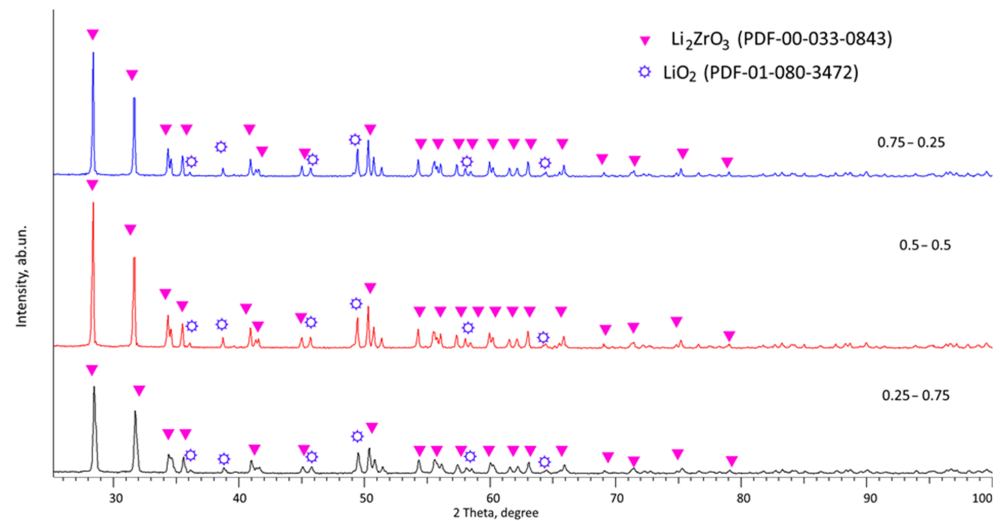


Figure 1. Results of X-ray phase analysis of the studied samples of lithium-containing ceramics depending on the variation in the concentration of the initial components.

Table 1. Data from phase analysis and structural parameters of the studied ceramics obtained from composition 1.

0.25–0.75	0.5–0.5	0.75–0.25
Li_2ZrO_3 Monoclinic, C2/c(15) (PDF-00-033-0843)		
$a = 5.3936 \text{ \AA}, b = 8.9584 \text{ \AA}, c = 5.3201 \text{ \AA}, \beta = 112.477^\circ, V = 237.53 \text{ \AA}^3$	$a = 5.3883 \text{ \AA}, b = 8.9548 \text{ \AA}, c = 5.3191 \text{ \AA}, \beta = 112.387^\circ, V = 237.30 \text{ \AA}^3$	$a = 5.3839 \text{ \AA}, b = 8.9477 \text{ \AA}, c = 5.3148 \text{ \AA}, \beta = 112.297^\circ, V = 236.89 \text{ \AA}^3$
LiO_2 Orthorhombic, Pnm(58) (PDF-01-080-3472)		
$a = 3.9875 \text{ \AA}, b = 4.8722 \text{ \AA}, c = 2.9581 \text{ \AA}, V = 57.37 \text{ \AA}^3$	$a = 3.9803 \text{ \AA}, b = 4.8742 \text{ \AA}, c = 2.9558 \text{ \AA}, V = 57.34 \text{ \AA}^3$	$a = 3.9771 \text{ \AA}, b = 4.8683 \text{ \AA}, c = 2.9534 \text{ \AA}, V = 57.18 \text{ \AA}^3$

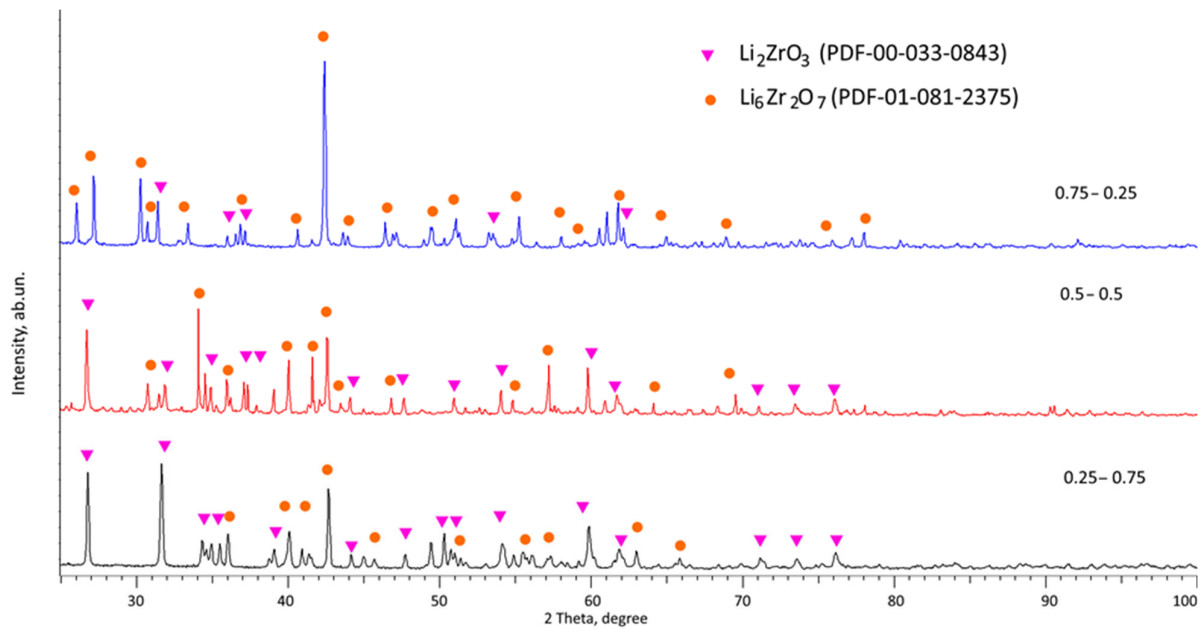


Figure 2. Results of X-ray phase analysis of the studied samples of lithium-containing ceramics depending on the variation in the concentration of the initial components.

Table 2. Data from phase analysis and structural parameters of the studied ceramics obtained from composition 2.

0.25–0.75	0.5–0.5	0.75–0.25
Li₂ZrO₃ Monoclinic, C2/c(15) (PDF-00-033-0843)		
$a = 5.3953 \text{ \AA}, b = 9.0068 \text{ \AA}, c = 5.3889 \text{ \AA}, \beta = 112.414^\circ, V = 242.09 \text{ \AA}^3$	$a = 5.4006 \text{ \AA}, b = 8.9803 \text{ \AA}, c = 5.3773 \text{ \AA}, \beta = 112.171^\circ, V = 241.51 \text{ \AA}^3$	$a = 5.3826 \text{ \AA}, b = 8.9645 \text{ \AA}, c = 5.3657 \text{ \AA}, \beta = 111.973^\circ, V = 240.10 \text{ \AA}^3$
Li₆Zr₂O₇ Monoclinic, C2/c(15) (PDF-01-081-2375)		
$a = 10.4216 \text{ \AA}, b = 5.9710 \text{ \AA}, c = 10.1699 \text{ \AA}, \beta = 99.994^\circ, V = 623.25 \text{ \AA}^3$	$a = 10.3909 \text{ \AA}, b = 5.9559 \text{ \AA}, c = 10.2358 \text{ \AA}, \beta = 99.975^\circ, V = 623.88 \text{ \AA}^3$	$a = 10.3644 \text{ \AA}, b = 5.9336 \text{ \AA}, c = 10.1937 \text{ \AA}, \beta = 100.034^\circ, V = 617.31 \text{ \AA}^3$

The main difference in the use of lithium-containing components in the form of Li₂CO₃ and LiClO₄·3H₂O is that when lithium carbonate is used, the phase composition of the ceramics is presented in the form of two monoclinic phases Li₂ZrO₃ and Li₆Zr₂O₇, the contributions of which vary with changes in the concentration of lithium carbonate. Moreover, in the case of using lithium perchlorate, the dominant phase in the composition of the resulting ceramics is the monoclinic phase Li₂ZrO₃, and also in the composition of the ceramics, the presence of impurity inclusions in the form of the orthorhombic phase LiO₂ is observed, the content of which varies from 1.4 to 7.3 wt%.

Figure 3 depicts the results concerning the variations in the strength characteristics of the lithium-containing ceramics studied. These ceramics were obtained from different compositions where the components were altered to achieve two-phase ceramics. The general trend observed in the strength parameter data indicates a favorable impact from

the introduction of impurity phases, such as LiO_2 (for composition 1) and $\text{Li}_6\text{Zr}_2\text{O}_7$ (for composition 2). Furthermore, in the case of composition 2, where $\text{Li}_6\text{Zr}_2\text{O}_7$ predominates in the composition of the ceramic, a more noticeable shift in strength parameters is observed. This can be attributed to the effects of structural ordering, which ranges from 89% to 93% in ceramic samples. Additionally, the formation of interphase boundaries hinders the propagation of microcracks and fractures within the ceramics. Moreover, in the case of using composition 1, the formation of the LiO_2 impurity phase at high concentrations of the lithium-containing component $\text{LiClO}_4 \cdot 3\text{H}_2\text{O}$ leads to maximum strengthening of no more than 7–8%, while when using composition 2, strengthening and resistance to cracking under external load exceeds 9–11%.

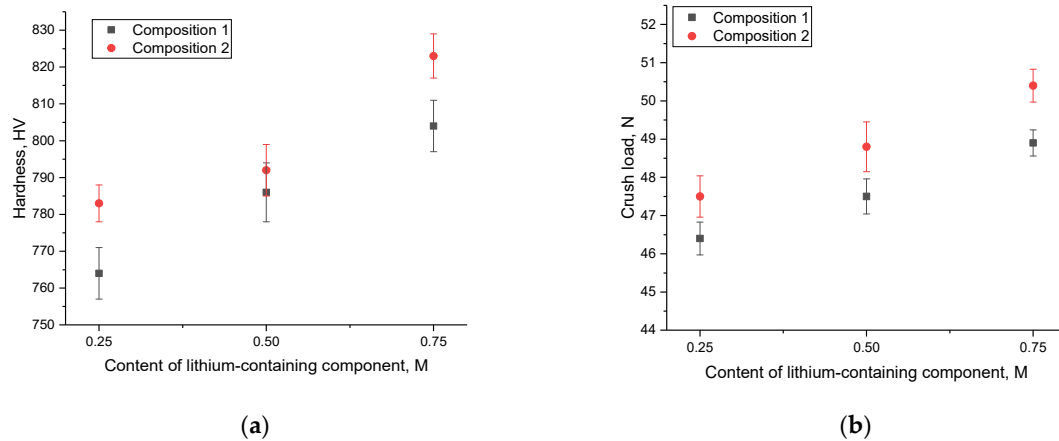


Figure 3. Results of changes in the strength parameters of lithium-containing ceramics depending on the concentration of the lithium-containing component: (a) results of changes in hardness and (b) results of changes in resistance to single compression at a compression speed of 0.1 mm/min.

Figure 4 demonstrates the results of a comparative analysis of alterations in the strengthening efficiency of ceramics obtained from different compositions, depending on the concentration of the impurity phase (in the case of composition 1— LiO_2 phase, in the case of composition 2— $\text{Li}_6\text{Zr}_2\text{O}_7$ phase). As a comparison, the values of hardness and resistance of ceramics to cracking under single compression were taken from works [28,29]. The hardening values were calculated taking into account changes in hardness values and the maximum pressure that the ceramics could withstand during a single compression at a speed of 0.1 mm/min. The overall trend observed in the data suggests that the most significant alterations in the strength characteristics of ceramics due to variations in impurity inclusions occur at low concentrations. This is true for ceramics obtained from both composition 1 and composition 2. Furthermore, in the case of composition 2, when the $\text{Li}_6\text{Zr}_2\text{O}_7$ phase dominates at high concentrations, the strengthening effect is minimal, not exceeding 10%. This can be attributed to the dominance of the $\text{Li}_6\text{Zr}_2\text{O}_7$ phase in the ceramic composition, which results in a reduction of its strengthening properties. The strengthening effect in ceramics resulting from an increase in impurity inclusions is attributed to the presence of interphase boundaries. A higher concentration of these boundaries hinders the propagation of microcracks and cleavages under external loads and compression of the samples. However, when the $\text{Li}_6\text{Zr}_2\text{O}_7$ phase prevails in the ceramic composition, a slight decrease in the rate of strength characteristics' growth is observed. This can be explained by the dominance of this phase, which has lower strength and a decrease in interphase boundaries. Thus, by analyzing the general alterations in strength characteristics depending on the production conditions (i.e., with variations in the ratio of the initial components), the following conclusion can be drawn. The formation of impurity inclusions in the form of LiO_2 or $\text{Li}_6\text{Zr}_2\text{O}_7$ results in a growth in strength characteristics (hardening of ceramics), which can be explained by the effects of interphase boundaries, the formation of which leads to a rise in resistance to cracking under external mechanical

influences. In this case, the most pronounced changes are observed for two-phase ceramics, in which the $\text{Li}_6\text{Zr}_2\text{O}_7$ phase dominates.

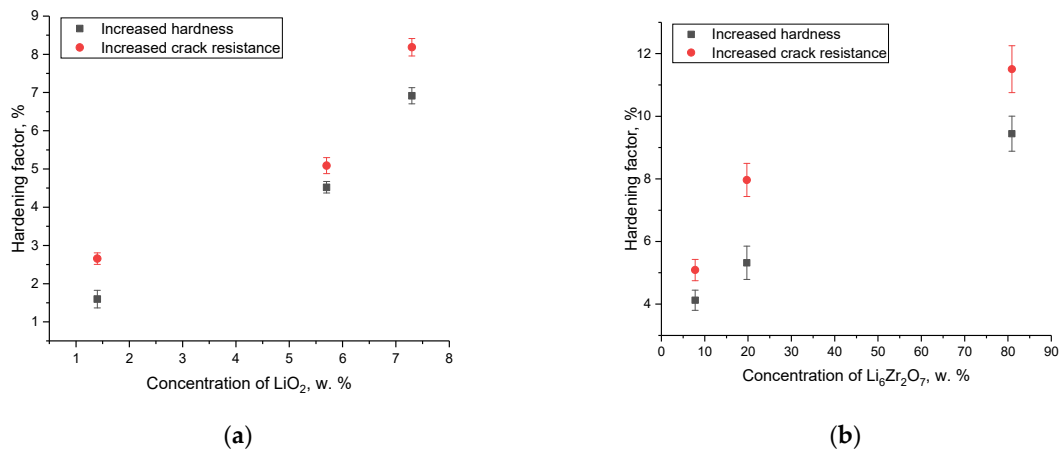


Figure 4. Results of strengthening depending on the concentration of impurity phases: (a) when changing the concentration of LiO_2 and (b) when changing the concentration of $\text{Li}_6\text{Zr}_2\text{O}_7$.

A change in the speed of mechanical influence on samples leads to an acceleration of the propagation of microcracks in the samples, which in turn leads to accelerated cracking at lower values of external load. In this case, the accelerated mechanical impact on the samples leads to the rapid spread of deformations and an increase in stress in the samples, which is accompanied by an acceleration of the destructive propagation of cracks. The results of experiments on changing the loading rate on samples under single compression are presented in Figure 5. The compression rate varied within the range of 0.1 mm/min, 0.3 mm/min, 0.5 mm/min, 1 mm/min, and 2 mm/min.

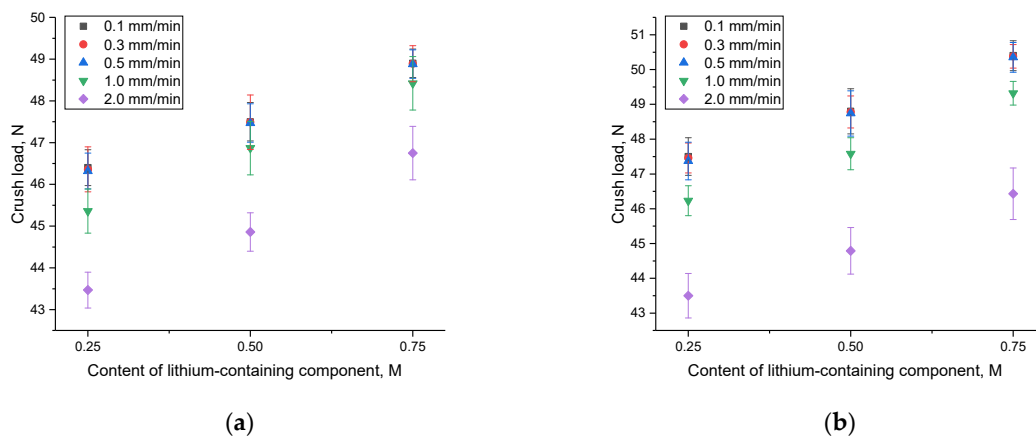


Figure 5. Results of tests on the crack resistance of ceramics when changing the rate of single compression in the case of varying ceramic compositions: (a) composition 1 and (b) composition 2.

An examination of the data displayed in Figure 5 revealed that at low compression rates, there are minimal alterations in the crack resistance value (the maximum pressure ceramics can endure during a single compression). This suggests that ceramics exhibit remarkable resistance to minor fluctuations in the speed of external influences. However, as the compression rate escalates, a reduction in crack resistance becomes evident (refer to Figure 6), signifying that at elevated rates of external influences, there is a rapid surge in the propagation of microcracks and structural deformations, resulting in cracking at lower load values. It is worth mentioning that when the concentration of impurity inclusions increases, a reduction in the extent of changes in crack resistance at high speeds is evident. This signifies a favorable trend in the impact of interphase boundaries on resistance to structural deformations under external loads and underscores the enhanced

stability of ceramics' strength properties. Additionally, an analysis of these variations, as depicted in Figures 5 and 6, highlights that the ceramics obtained from composition 1 exhibit the highest resistance to external influences. This is evident as the decline in resistance to external influences under heavy loads is less pronounced for them.

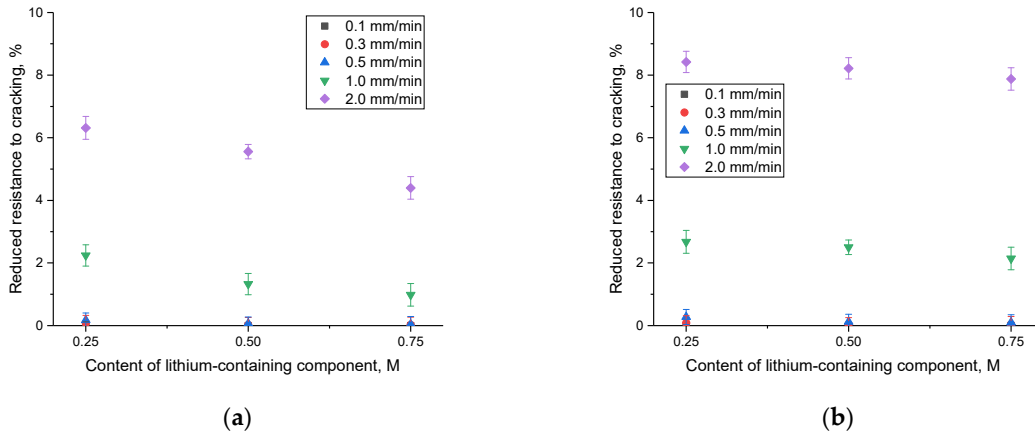


Figure 6. Results of changes in cracking resistance with changes in compression rate: (a) composition 1 and (b) composition 2.

An evaluation of the thermal conductivity variation in ceramics concerning different compositions and component concentrations is depicted in Figure 7. These measurements encompassed a temperature range from 25 to 700 °C and employed the longitudinal thermal conductivity flow measurement method. It is noteworthy that the increase in temperature from 25 to 700 °C did not yield substantial alterations in the thermal conductivity coefficient. This underscores the remarkable stability of thermophysical parameters across the entire temperature range under consideration.

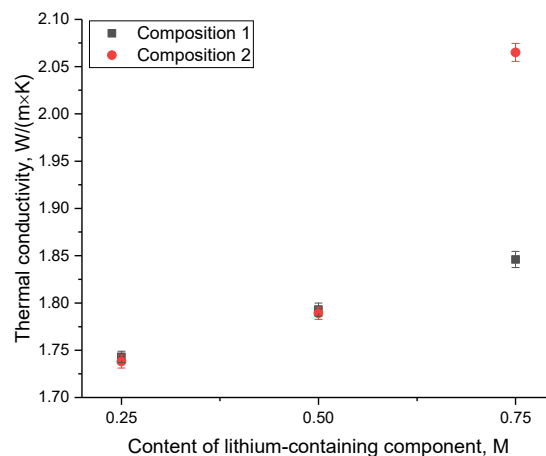


Figure 7. Results of changes in the thermal conductivity coefficient of the studied ceramics depending on changes in the concentration of lithium-containing components.

As evident from the data presented, the variations in the thermal conductivity coefficient are indicative of the beneficial impact of minor impurity inclusions, which contribute to an increase in thermal conductivity. When using Li_2CO_3 as the lithium-containing component at elevated concentrations, leading to the dominance of the $\text{Li}_6\text{Zr}_2\text{O}_7$ phase, a marked escalation in thermal conductivity is observed in comparison to composition 1. This decrease can be elucidated by the predominance of the $\text{Li}_6\text{Zr}_2\text{O}_7$ phase, characterized by superior thermal conductivity properties when contrasted with the Li_2ZrO_3 phase [30]. It is noteworthy that the thermal conductivity values for the acquired ceramic samples surpass the thermal conductivity values of analogous samples obtained through the Hot

Wire Method [31]. These disparities can be ascribed to not only the presence of interphase boundaries but also an upsurge in the degree of structural ordering. A modification in the degree of structural ordering results in fewer structural deformations in the crystal lattice, subsequently leading to a reduction in the defective inclusions that impede phonon heat transfer.

One of the important parameters for assessing the resistance of ceramics to external influences is the determination of their resistance to external influences under conditions of elevated temperatures corresponding to conditions as close as possible to operating conditions. Under such circumstances, the impact on the samples may be more severe, given that the ceramic specimens are subject to thermal expansion. This, in turn, can have adverse effects on the ceramics' strength properties and stability dynamics. The experiments were conducted using a testing apparatus equipped with a heating chamber, which facilitates the heating of samples up to 500 °C, enabling temperature stabilization, followed by a single compression test. Figure 8 illustrates a comparative assessment of variations in the resistance to single compression, both at room temperature and at 500 °C, offering insights into the data related to resistance to external forces.

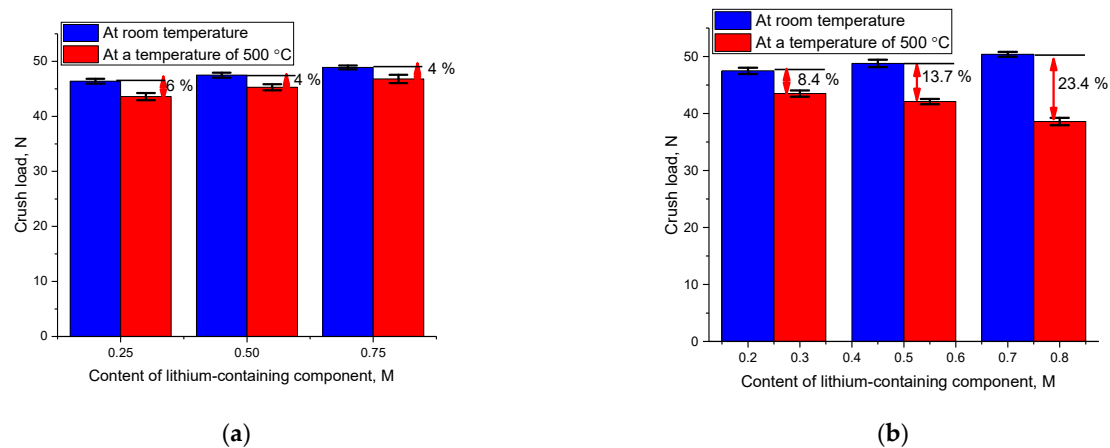


Figure 8. Results of a study of resistance to single compression at different temperatures of lithium-containing ceramics: (a) composition 1 and (b) composition 2.

The data presented indicate that when dealing with ceramics containing the LiO_2 impurity phase, raising the testing temperature from room temperature to 500 °C results in a minor reduction in the resistance to single compression (within a range of 4–6%). Furthermore, an increase in the concentration of the LiO_2 impurity phase diminishes the disparities in the data concerning variations in resistance to single compression, which can be attributed to heightened resistance to thermal expansion of ceramics when subjected to heat. For two-phase ceramics of the $\text{Li}_2\text{ZrO}_3/\text{Li}_6\text{Zr}_2\text{O}_7$ composition, an elevated concentration of the $\text{Li}_6\text{Zr}_2\text{O}_7$ phase with rising test temperatures during single compression results in a significant decrease in stability. This phenomenon can be attributed to variations in the thermal expansion of the crystal lattice, alongside a reduced resistance of ceramics to external forces stemming from thermal expansion.

Figure 9 shows the results of changes in the value of volumetric expansion of samples after thermal tests for resistance to long-term temperature heating of 500 h.

The data analysis reveals that an increase in the concentration of impurity inclusions in the form of the LiO_2 phase in the ceramic composition leads to enhanced stabilization of the crystal lattice's thermal expansion. This is substantiated by the findings on the stability of strength characteristics, as shown in Figure 9b. Conversely, the prevalence of the $\text{Li}_6\text{Zr}_2\text{O}_7$ phase in the ceramic composition (derived from composition 2) disrupts both thermal stability (significantly elevating the coefficient of volumetric thermal expansion by over 1.5 times) and the hardness of the ceramics. These findings indicate a decline in strength characteristics' stability during high-temperature aging.

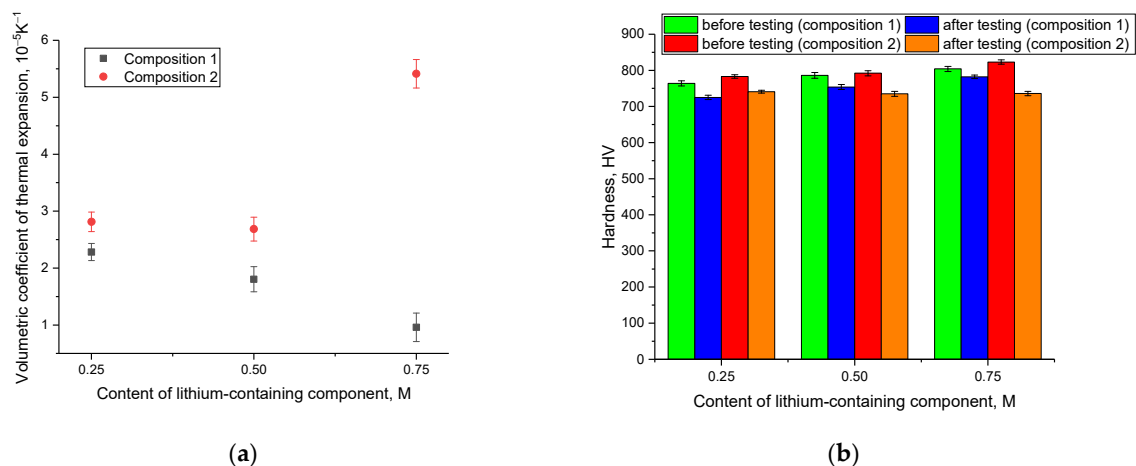


Figure 9. (a) Results of changes in the coefficient of volumetric thermal expansion and (b) results of changes in hardness values of ceramic samples after thermal stability tests.

In the case of two-phase ceramics, it was found that an increase in the contribution of the $\text{Li}_6\text{Zr}_2\text{O}_7$ phase leads to increased stability to high-temperature aging and degradation, due to increased stability to softening, as well as a decrease in the effect of thermal volumetric expansion of the crystal structure. In turn, the increase in resistance to cracking during long-term high-temperature degradation (high-temperature aging) for two-phase ceramics in the case of the dominance of the $\text{Li}_6\text{Zr}_2\text{O}_7$ phase can be explained by interphase boundaries, the presence of which is an obstacle to the propagation of microcracks under external influences (mechanical pressure), and the presence of interphase boundaries leads to an increase in resistance to volumetric thermal expansion of the crystal structure as a result of prolonged thermal effects.

4. Conclusions

During the X-ray phase analysis studies, it was determined that incorporating $\text{LiClO}_4 \cdot 3\text{H}_2\text{O}$ as a lithium-containing component in the ceramic manufacturing process results in the formation of a predominant monoclinic phase, Li_2ZrO_3 , with impurity inclusions in the shape of the LiO_2 orthorhombic phase. The maximum proportion of LiO_2 impurity does not surpass 7–8%. Conversely, when employing Li_2CO_3 as the lithium-containing component in ceramics production using the proposed methodology, it was possible to create two-phase ceramics composed of monoclinic phases, Li_2ZrO_3 and $\text{Li}_6\text{Zr}_2\text{O}_7$. Analysis of mechanical tests revealed a positive effect of impurity inclusions on resistance to mechanical tests and an increase in hardness, both at room temperatures and during long-term high-temperature aging. The change in resistance to mechanical damage (under single compression) is due to the presence of impurity inclusions, an increase in the concentration of which leads to an increase in the contribution of interphase boundaries that prevent the propagation of microcracks in the samples.

The potential for practical application of the research results obtained consists of the proposed technology for creating lithium-containing ceramics by simple and inexpensive mechanochemical solid-phase synthesis combined with thermal annealing of the resulting powders. Moreover, the use of the proposed technology for creating ceramics by varying different concentrations of the initial components makes it possible to obtain ceramics with a given phase composition, the alteration of which affects the strengthening and increasing the resistance of ceramics to external influences.

Author Contributions: Conceptualization, B.K.A., S.G.G. and A.L.K.; methodology, B.K.A., S.G.G. and A.L.K.; formal analysis, B.K.A., S.G.G. and A.L.K.; investigation, B.K.A., S.G.G. and A.L.K.; resources, B.K.A., S.G.G. and A.L.K.; writing—original draft preparation, review, and editing, B.K.A., S.G.G. and A.L.K.; visualization, B.K.A., S.G.G. and A.L.K.; supervision, B.K.A., S.G.G. and A.L.K. All authors have read and agreed to the published version of the manuscript.

Funding: The work was supported by the Science Committee of the Ministry of Science and Higher Education of the Republic of Kazakhstan (Grant No. AP14972969).

Institutional Review Board Statement: Not applicable.

Informed Consent Statement: Not applicable.

Data Availability Statement: Data are contained within the article.

Conflicts of Interest: The authors declare no conflict of interest.

References

1. Zhiznin, S.; Timokhov, V.; Gusev, A. Economic aspects of nuclear and hydrogen energy in the world and Russia. *Int. J. Hydrog. Energy* **2020**, *45*, 31353–31366. [[CrossRef](#)]
2. Singh, S.; Jain, S.; Ps, V.; Tiwari, A.K.; Nouni, M.R.; Pandey, J.K.; Goel, S. Hydrogen: A sustainable fuel for future of the transport sector. *Renew. Sustain. Energy Rev.* **2015**, *51*, 623–633. [[CrossRef](#)]
3. Maczulak, A.E. *Renewable Energy: Sources and Methods*; Infobase Publishing: New York, NY, USA, 2010.
4. Revankar, S.T. Nuclear hydrogen production. In *Storage and Hybridization of Nuclear Energy*; Academic Press: New York, NY, USA, 2019; pp. 49–117.
5. Mathew, M.D. Nuclear energy: A pathway towards mitigation of global warming. *Prog. Nucl. Energy* **2022**, *143*, 104080. [[CrossRef](#)]
6. Kulsartov, T.; Zaurbekova, Z.; Knitter, R.; Shaimerdenov, A.; Chikhray, Y.; Askerbekov, S.; Ponkratov, Y. Studies of two-phase lithium ceramics $\text{Li}_4\text{SiO}_4\text{-Li}_2\text{TiO}_3$ under conditions of neutron irradiation. *Nucl. Mater. Energy* **2022**, *30*, 101129. [[CrossRef](#)]
7. Tan, G.; Song, S.; Hu, X.; Cai, L.; Li, Y.; Zhang, Y. Efficient fabrication of high strength Li_2TiO_3 ceramic pebbles via improved rolling ball method assisted by sesbania gum binder. *Ceram. Int.* **2021**, *47*, 26978–26990. [[CrossRef](#)]
8. Tan, G.; Hu, X.; Wang, S.; Yang, X.; Li, Y.; Yang, Z.; Zhang, Y. A process for fabrication of Li_2TiO_3 ceramic pebbles with high mechanical properties via non-hydrolytic sol-gel method. *Ceram. Int.* **2020**, *46*, 27686–27694. [[CrossRef](#)]
9. Kolb, M.; Knitter, R.; Hoshino, T. Li_4SiO_4 based breeder ceramics with Li_2TiO_3 , LiAlO_2 and LiXLaYTiO_3 additions, part II: Pebble properties. *Fusion Eng. Des.* **2017**, *115*, 6–16. [[CrossRef](#)]
10. Xiang, M.; Zhang, Y.; Wang, C.; Zhang, Y.; Liu, W.; Li, G. Preparation of $\text{Li}_4\text{SiO}_{4-x}\text{Li}_2\text{O}$ powders and pebbles for advanced tritium breeders. *Ceram. Int.* **2017**, *43*, 2314–2319. [[CrossRef](#)]
11. Guo, H.; Wang, H.; Chen, R.; Gong, Y.; Yang, M.; Ye, D.; Shi, Y.; Shi, Q.; Lu, T. Characterization of Li-rich Li_2TiO_3 ceramic pebbles prepared by rolling method sintered in air and vacuum. *J. Nucl. Mater.* **2021**, *546*, 152786. [[CrossRef](#)]
12. Cai, L.; Hu, X.; Tan, G.; Li, G.; Zhang, Y. Accurate and uniform fabrication of Li_2TiO_3 pebbles with high properties based on Stereolithography technology. *J. Eur. Ceram. Soc.* **2021**, *41*, 2114–2123. [[CrossRef](#)]
13. Yang, L.; Li, Z.; Gao, C.; Gong, S.; Chen, J.; Chen, H.; Zhang, H. Li_2ZrO_3 based Li-ion conductors doped with halide ions & sintered in oxygen-deficient atmosphere. *Ceram. Int.* **2021**, *47*, 31907–31914.
14. Bi, J.; Xing, C.; Yang, C.; Wu, H. Phase composition, microstructure and microwave dielectric properties of rock salt structured $\text{Li}_2\text{ZrO}_3\text{-MgO}$ ceramics. *J. Eur. Ceram. Soc.* **2018**, *38*, 3840–3846. [[CrossRef](#)]
15. Yang, L.; Zhang, H.; Chen, J.; Chen, H.; Li, Z. Electrical conductivity of Al-doped Li_2ZrO_3 ceramics for Li-ion conductor electrolytes. *Ceram. Int.* **2021**, *47*, 17950–17955. [[CrossRef](#)]
16. Gong, Y.; Yang, M.; Feng, L.; Shi, Q.; Shi, Y.; Xiang, X.; Huang, Z.; Wei, J.; Lu, T.; Huang, W. Fabrication of attractive Li_4SiO_4 pebbles with modified powders synthesized via surfactant-assisted hydrothermal method. *Ceram. Int.* **2016**, *42*, 10014–10020. [[CrossRef](#)]
17. Yang, M.; Gong, Y.; Yu, X.; Feng, L.; Shi, Y.; Huang, Z.; Xiang, X.; Wei, J.; Lu, T. Fabrication of Li_4SiO_4 ceramic pebbles with uniform grain size and high mechanical strength by gel-casting. *Ceram. Int.* **2016**, *42*, 2180–2185. [[CrossRef](#)]
18. Hu, X.; Tan, G.; Cai, L.; Song, S.; Wu, W.; Feng, B.; Qin, Z.; Liu, R.; Shen, Z.; Zhang, Y. A novel process for fully automatic mass-production of Li_2TiO_3 ceramic pebbles with uniform structure and size. *Ceram. Int.* **2022**, *48*, 6393–6401. [[CrossRef](#)]
19. Rao, G.J.; Mazumder, R.; Bhattacharyya, S.; Chaudhuri, P. Fabrication of $\text{Li}_4\text{SiO}_4\text{-Li}_2\text{ZrO}_3$ composite pebbles using extrusion and spherodization technique with improved crush load and moisture stability. *J. Nucl. Mater.* **2019**, *514*, 321–333.
20. Gabriel, O.N.; Martina, G.; Gabriel, L.; Gustavo, S. Dense m- Li_2ZrO_3 formed by aqueous slip casting technique: Colloidal and rheological characterization. *Ceram. Int.* **2023**, *49*, 8827–8838. [[CrossRef](#)]
21. Paudel, H.P.; Duan, Y. A first-principles density function theory study of tritium diffusion in Li_2ZrO_3 : Application for producing tritium. *J. Phys. Chem. C* **2018**, *122*, 28447–28459. [[CrossRef](#)]
22. Beloglazov, S.; Nishikawa, M.; Tanifuji, T. Modelling of tritium release from irradiated Li_2ZrO_3 . *Fusion Sci. Technol.* **2002**, *41*, 1049–1053. [[CrossRef](#)]
23. Kenzhina, I.; Kulsartov, T.; Knitter, R.; Chikhray, Y.; Kenzhin, Y.; Zaurbekova, Z.; Nesterov, E. Analysis of the reactor experiments on the study of gas evolution from two-phase $\text{Li}_2\text{TiO}_3\text{-Li}_4\text{SiO}_4$ lithium ceramics. *Nucl. Mater. Energy* **2022**, *30*, 101132. [[CrossRef](#)]
24. Avila, R.; Peña, L.; Jiménez, J. Surface desorption and bulk diffusion models of tritium release from Li_2TiO_3 and Li_2ZrO_3 pebbles. *J. Nucl. Mater.* **2010**, *405*, 244–251. [[CrossRef](#)]

25. Chattaraj, D. Structural, electronic, elastic and thermodynamic properties of Li_2ZrO_3 : A comprehensive study using DFT formalism. *J. Nucl. Mater.* **2017**, *496*, 286–292. [[CrossRef](#)]
26. Berguzinov, A.; Kozlovskiy, A.L.; Khametova, A.A.; Shlimas, D.I. Study of Structural and Strength Changes in Lithium-Containing Ceramics—Potential Blanket Materials for Nuclear Power, Subjected to High-Dose Proton Irradiation. *Materials* **2022**, *15*, 5572. [[CrossRef](#)] [[PubMed](#)]
27. Shlimas, D.I.; Borgekov, D.B.; Kozlovskiy, A.L.; Zdorovets, M.V. Synthesis and Structural and Strength Properties of $x\text{Li}_2\text{ZrO}_3-(1-x)\text{MgO}$ Ceramics—Materials for Blankets. *Materials* **2023**, *16*, 5176. [[CrossRef](#)] [[PubMed](#)]
28. Abyshev, B.; Shlimas, D.I.; Zdorovets, M.V.; Arshamov, Y.K.; Kozlovskiy, A.L. Study of radiation resistance to helium swelling of $\text{Li}_2\text{ZrO}_3/\text{LiO}$ and Li_2ZrO_3 ceramics. *Crystals* **2022**, *12*, 384. [[CrossRef](#)]
29. Kozlovskiy, A.L.; Abyshev, B.; Shlimas, D.I.; Zdorovets, M.V. Study of Structural, Strength, and Thermophysical Properties of $\text{Li}_{2+4x}\text{Zr}_{4-x}\text{O}_3$ Ceramics. *Technologies* **2022**, *10*, 58. [[CrossRef](#)]
30. Pfeiffer, H.; Bosch, P. Thermal stability and high-temperature carbon dioxide sorption on hexa-lithium zirconate ($\text{Li}_6\text{Zr}_2\text{O}_7$). *Chem. Mater.* **2005**, *17*, 1704–1710. [[CrossRef](#)]
31. Enoda, M.; Ohara, Y.; Roux, N.; Ying, A.; Pizza, G.; Malang, S. Effective Thermal Conductivity Measurement of the Candidate Ceramic Breeder Pebble Beds by the Hot Wire Method. *Fusion Technol.* **2001**, *39*, 612–616. [[CrossRef](#)]

Disclaimer/Publisher’s Note: The statements, opinions and data contained in all publications are solely those of the individual author(s) and contributor(s) and not of MDPI and/or the editor(s). MDPI and/or the editor(s) disclaim responsibility for any injury to people or property resulting from any ideas, methods, instructions or products referred to in the content.